Downloaded from http://iranpaper.ir
This article has been accepted for inclusion in a future issue of this journal. Content is final as presented, with the exception of pagination.

Networked Microgrids for Self-Healing Power Systems

Zhaoyu Wang, *Student Member, IEEE*, Bokan Chen, Jianhui Wang, *Senior Member, IEEE*, and Chen Chen, *Member, IEEE*

***Abstract*—This paper proposes a transformative architecture for the normal operation and self-healing of networked microgrids (MGs). MGs can support and interchange electricity with each other in the proposed infrastructure. The networked MGs are connected by a physical common bus and a designed two-layer cyber communication network. The lower layer is within each MG where the energy management system (EMS) schedules the MG operation; the upper layer links a number of EMSs for global optimization and communication. In the normal operation mode, the objective is to schedule dispatchable distributed generators (DGs), energy storage systems (ESs), and controllable loads to minimize the operation costs and maximize the supply adequacy of each MG. When a generation deficiency or fault happens in an MG, the model switches to the self-healing mode and the local generation capacities of other MGs can be used to support the on-emergency portion of the system. A consensus algorithm is used to distribute portions of the desired power support to each individual MG in a decentralized way. The allocated portion corresponds to each MG's local power exchange target, which is used by its EMS to perform the optimal schedule. The resultant aggregated power output of networked MGs will be used to provide the requested power support. Test cases demonstrate the effectiveness of the proposed methodology.**

***Index Terms*—Consensus algorithm, distributed power generation, microgrid (MG), power distribution faults, self-healing.**

NOMENCLATURE

Acronyms

WT	Wind turbine.
PV	Photovoltaic generator.
ES	Energy storage system.
MT	Micro turbine.
MG	Microgrid.

Indices

n	Index for MGs.
i	Index for nodes.
t	Index for time.
k	Iteration step in consensus algorithm.

Sets

G_n	Set of MTs in nth MG.
E_n	Set of nodes with nondispatchable DGs.
S_n	Set of nodes with energy storage system.
$D1_n/D2_n$	Set of noncontrollable/controllable load nodes in nth MG.
N_1/N_2	Set of MGs without faults/with faults.
M_n	Set of neighbors of nth MG.

Parameters

$F(\cdot)$	Generation cost function.
L^P/L^Q	Active/reactive demand, in MW/MVAR.
$\theta^{p,\max}/\theta^{q,\max}$	Maximum active/reactive power transfer, in MW/MVAR.
$P^{\max}/Q^{\max}$	Maximum active/reactive power outputs, in MW/MVAR.
$P^{\min}/Q^{\min}$	Minimum active/reactive power outputs, in MW/MVAR.
δ^p/δ^q	Active/reactive ramp limit, in MW/MVAR.
$P^{\mathrm{dch},\max}/P^{\mathrm{ch},\max}$	Maximum discharging/charging, in MW.
EC	Capacity of the energy storage, in MWh.
η_d/η_c	Discharging/charging efficiency.
$L^{P,\min}/L^{Q,\min}$	Minimum active/reactive demand of controllable load, in MW/MVAR.
T	Time interval between t and $t-1$, in hours.
T^c	Maximum time period with load control, in hours.
τ	Step size in consensus algorithm.
$t_{\min}/t_{\max}$	Start/end of time horizon.
ρ_e/ρ_l	Power exchange/load control penalty price, in \$/MW or \$/MVAR.

Variables

$P_{i(i\in G\cup S)}$	Power output of MTs/ESSs, in MW.
θ^p/θ^q	Active/Reactive power exchange, in MW/MVAR.

Manuscript received August 25, 2014; revised November 1, 2014, January 4, 2015, and March 15, 2015; accepted April 22, 2015. This work was supported by the U.S. Department of Energy Office of Electricity Delivery and Energy Reliability. Paper no. TSG-00844-2014.

Z. Wang is with the School of Electrical and Computer Engineering, Georgia Institute of Technology, Atlanta, GA 30332 USA (e-mail: zhaoyuwang@gatech.edu).

B. Chen is with the School of Industrial and Manufacturing Systems Engineering, Iowa State University, Ames, IA 50014 USA (e-mail: bokanc@iastate.edu).

J. Wang and C. Chen are with Argonne National Laboratory, Argonne, IL 60439 USA (e-mail: jianhui.wang@anl.gov; morningchen@anl.gov).

Color versions of one or more of the figures in this paper are available online at http://ieeexplore.ieee.org.

Digital Object Identifier 10.1109/TSG.2015.2427513

1949-3053 © 2015 IEEE. Personal use is permitted, but republication/redistribution requires IEEE permission.
See http://www.ieee.org/publications_standards/publications/rights/index.html for more information.

Downloaded from http://iranpaper.ir
This article has been accepted for inclusion in a future issue of this journal. Content is final as presented, with the exception of pagination.

v	Controllable load state (1-under control and 0-free of control).
P^D/Q^D	Adjusted active/reactive load, in MW/MVAR.
u	Commitment state of MTs.
x/y	Discharging/charging state of ES.
SoC	State of charge of ES.
Z^p/Z^q	Desired aggregated active/reactive demand output of MGs without faults, in MW/MVAR.
ψ^p/ψ^q	Total active/reactive support gap, in MW/MVAR.
λ^p/λ^q	Global active/reactive power ratio.
μ^p/μ^q	Desired active/reactive demand output of an MG without faults, in MW/MVAR.
B	Iteration variable.

I. Introduction

MICROGRID is a power distribution system integrating distributed generators (DGs), energy storage systems (ESs) and controllable loads [1], [2]. An MG can work in a grid-connected mode or an islanded mode. A smart MG is distinguished from the traditional distribution systems in terms of reliability, self-adequacy, self-healing, and interactive characteristics [3]. According to recent studies in [2]–[9], connecting multiple MGs to form a power system can further improve the system operation and reliability thanks to the salient features of networked MGs such as coordinated energy management and interactive support and exchange.

MGs are essential components of smart grids. Many studies have been made in the literature on various topics of MGs, such as planning [10], [11], energy management [1], [2], [4], [12]–[14], and service restoration [3], [15]. Wang *et al.* [10] proposed a robust optimization model and the corresponding solution algorithm for MG planning considering the uncertainties of DG outputs and load consumptions. Khodaei [1] proposed a model for MG optimal scheduling considering multiperiod islanding constraints based on Benders decomposition to decouple grid-connected operation and islanded operation. Jiang *et al.* [12] presented a two-layer dispatch framework coordinated through power reserve for MG operations in both grid-connected and islanded modes.

Connecting multiple MGs to construct networked MGs is the further development and application of the concept of MG. According to the IEEE Standard 1547.4 [16], the operation and reliability of a distribution system can be improved by splitting it into multiple MGs. Wang *et al.* [2] proposed a decentralized coordinated energy management system (EMS) of networked MGs in a distribution system considering the uncertain DG outputs and load consumption. Marvasti *et al.* [4] considered the distribution system and the connected multiple MGs as independent systems. A hierarchical optimization framework was developed to coordinate the optimal operation of the entire system. Wu and Guan [7] applied a dynamic programming algorithm and a decentralized partially-observable Markov decision process to solve the economic operation problems of networked MGs. Asimakopoulou *et al.* [8] presented a leader–follower model and a bi-level program for the energy management of networked MGs. Fathi and Bevrani [9] proposed an online stochastic algorithm for the energy consumption scheduling of networked MGs considering probabilistic demand.

Self-healing aided by MGs is an important feature of smart grids. Moreira *et al.* [15] developed the control framework for blackstart by using MGs. Arefifar *et al.* [3] proposed a planning model to divide a distribution system into networked MGs for its optimal self-healing. Wang and Wang [17] proposed a strategy to sectionalize the on-outage portion of a distribution system into multiple MGs to increase the grid resilience. Arefifar *et al.* [5] presented an optimal model to increase the reliability of a distribution system by dividing it into multiple MGs. However, it can be seen that the concept of using local MG generation capacities to support other MGs for the self-healing of a networked-MG system is not considered in the above literature. Moreover, the required decentralized cyber communication and control framework needs to be studied.

This paper proposes a transformative architecture for the optimal operation and self-healing of autonomous networked MGs. We consider the scenario that multiple MGs are physically connected via a common bus. For the purpose of information exchange and coordinated control, the MGs are also connected through a cyber communication network. In the normal operation mode, each MG operates independently. The operation costs and supply adequacy of each MG are optimized by controlling dispatchable DGs, ESs, and loads. When a fault or generation deficiency happens in an MG, the framework enters the self-healing mode. The on-emergency MG receives power support from other MGs that are under normal operation.

In order to coordinate the self-healing process in a decentralized fashion, a two-layer cyber communication and control network is developed. The lower-layer cyber network is within each MG, where the local EMS controls DGs, ESs and loads. The upper-layer network is composed of multiple EMSs. Each EMS only communicates with its neighboring counterparts. When an emergency occurs, the on-emergency MG broadcasts its requested power support in the cyber network. An average consensus algorithm is applied to allocate the desired power support among all normally-operating MGs. As an effective distributed mechanism, the average consensus algorithm has been well studied and verified [18]–[20]. The allocation determines the power support share of each MG, which will be used by the local EMS in each MG to perform the corresponding optimal dispatch. Finally, the aggregated power output from the normally-operating MGs will closely match the requested power support.

The remainder of this paper is organized as follows. Section II presents the proposed concept of networked MGs and the decentralized communication method. Section III proposes the formulations of the optimal normal operation and the self-healing problem. In Section IV, the numerical results are provided. Section V concludes this paper with the major findings.

Downloaded from http://iranpaper.ir
This article has been accepted for inclusion in a future issue of this journal. Content is final as presented, with the exception of pagination.

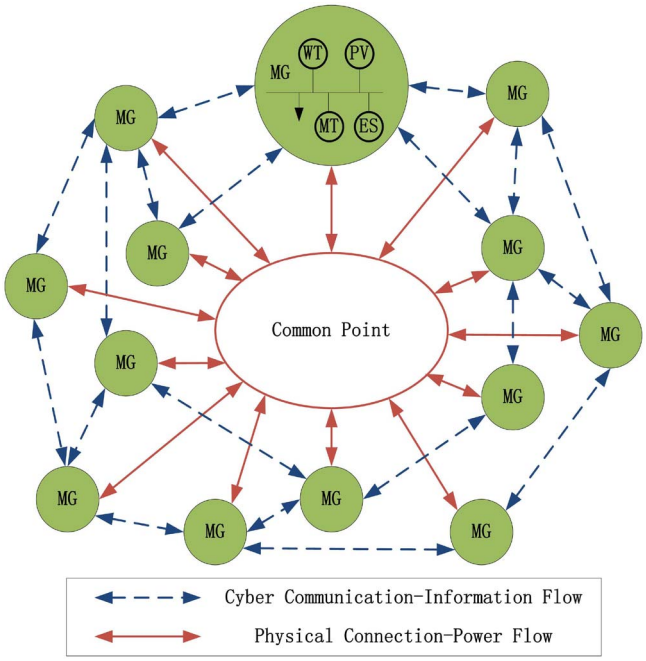

Fig. 1. Concept of networked MGs.

II. Networked Microgrids

Fig. 1 shows the autonomous networked MGs where utilities are not accessible or lost (e.g., utility grids or supplies are down). The interconnected MGs can support each other with local generation capacities to achieve the overall reliability. The network consists of both cyber links for communication and physical connections via a common point for power exchange. It is assumed that the cyber network is strongly connected, i.e., no island exists in the cyber network [20], [21]. In the normal operation mode, each MG works independently to fulfill its economic and self-adequate objectives. Details will be discussed in Section III. In this paper, generation deficiency and faults such as loss of generators and distribution lines are all considered as an emergency. In the self-healing mode, the on-emergency MG will receive power support from other MGs under normal operation until the emergency is cleared. We assume that the networked MGs have already been synchronized in the self-healing mode. The isolation and clearance of a fault is beyond this paper. Since there is no central controller and each MG only exchanges information with its neighboring counterparts via cyber links, the challenge is to inform each normally-operating MG the amount of power support requested and perform corresponding dispatch.

We propose a decentralized communication and control protocol for the networked MGs. The communication framework can be divided into two layers. The lower-layer cyber network is for each MG where a local EMS is installed to schedule the operation of DGs, ESs and loads within the MG. There are two types of DGs: 1) dispatchable DGs such as MTs; and 2) nondispatchable DGs such as PVs and WTs. It is assumed that all of the renewable generation will be taken by the power system. Loads can also be categorized into controllable loads and noncontrollable ones. The upper-layer cyber network is designed for the information exchange of the EMSs. There is no central controller in this network. Each EMS only communicates with its neighboring EMSs. It is assumed that each pair of EMSs with a direct cyber link has the two-way communication capability [20].

Under the normal operation, each MG is working in the autonomous mode, i.e., the self-adequate MG can autonomously provide reliable power supply to its customers without power exchange with utility grids or other MGs. Here, self-adequacy refers to the generation-load balance within an MG. Thus, no information exchange or power flow exchange is needed among MGs. The upper-layer network is idle in this mode. Operating MGs in the self-adequate mode can improve the operation, protection, and reliability of the system [3], [5], [9], [22]. In the self-healing mode, the on-emergency MG will receive power support from other MGs. A power support request will come from the on-emergency MG. The main idea is to allocate the desired power support to each normally-operating EMS as a local power exchange (power output to the common bus) target, via decentralized coordination among EMSs using the upper-layer cyber network. The actual aggregated support can approach the requested amount if each supporting MG controls its operation according to the allocated power support request.

There are two steps in the communication protocol for the normal operation mode: demand and supply information update (DSIU) and decision making in normal operation (DMNO). In the DSIU, the EMS at the lower-layer cyber network receives the generation information from DGs and ESs, and the demand information from the loads. With the collected data, the EMS updates the DG and ES outputs, load consumptions, ramp limits of MTs, and discharging and charging limits of ESs. In the DMNO, the EMS of an MG makes decisions to optimally schedule the DGs, ESs, and loads. Details can be found in Section III. Three steps exist in the communication protocol for the self-healing mode: DSIU, target power exchange update (TPEU) and decision making in self-healing (DMSH). During the TPEU, the upper-layer cyber interface module at each EMS communicates with its neighboring EMSs to compute the local power exchange target using the generation and supply information obtained in DSIU. An average consensus algorithm is applied to allocate the desired power support request to each MG in a distributed fashion. In the DMSH, the EMS performs optimal controls of DGs, ESs, and loads given the local power exchange target. The decisions will be broadcasted by the lower-layer cyber interface module at the end of the phase.

When a fault or generation deficiency happens in an MG, the on-emergency MG will increase the outputs of its dispatchable DGs to the maximum possible levels, and calculate requested support based on the outputs of dispatchable and nondispatchable DGs. The total active power support required by the on-emergency MG Z_t^p should be shared by MGs under normal operation. The local active power exchange target of the nth MG $\mu_{n,t}^p$ should reflect the required aggregated power support and load-generation status specified by Z_t^p, $\sum_{n\in N_1}\sum_{i\in G_n\cup E_n} P_{i,t}$ and $\sum_{n\in N_1}\sum_{i\in D_{1n}\cup D_{2n}}(L_{i,t}^P + P_{i,t}^D)$.

Downloaded from http://iranpaper.ir
This article has been accepted for inclusion in a future issue of this journal. Content is final as presented, with the exception of pagination.

Thus, we define the total active power support gap as

$$\psi_t^p = Z_t^p - \sum_{n\in N_1}\left(\sum_{i\in G_n\cup E_n} P_{i,t} - \sum_{i\in D_{1n}\cup D_{2n}}\left(L_{i,t}^P + P_{i,t}^D\right)\right). \quad (1)$$

One basic principle of the self-healing is that the MGs in normal operation should not sacrifice their load to support the on-emergency MGs. Thus, it is assumed that the load adjustment is temporarily blocked for MGs in normal operation. $\psi > 0$ indicates that the generators need to increase the output and the ESs should work in the discharging mode and increase the output. We define λ_t^p as the ratio of the total demand target gap to the maximum adjustable generation

$$\lambda_t^p = \frac{Z_t^p - \sum_{n\in N_1}\left(\sum_{i\in G_n\cup E_n} P_{i,t} - \sum_{i\in D_{1n}\cup D_{2n}}\left(L_{i,t}^P + P_{i,t}^D\right)\right)}{\sum_{n\in N_1}\left(\sum_{i\in G_n}\delta_i^p + \sum_{i\in S_n} P_i^{\mathrm{dch,max}}\right)}. \quad (2)$$

The nth normally-operating MG applies the above ratio to set its local target power exchange with the common point as follows:

$$\mu_{n,t}^p = \sum_{i\in G_n\cup E_n} P_{i,t} + \lambda_t^p\left(\sum_{i\in G_n}\delta_i + \sum_{i\in S_n} P_i^{\mathrm{dch,max}}\right) - \sum_{i\in D_{1n}\cup D_{2n}}\left(L_{i,t}^P + P_{i,t}^D\right). \quad (3)$$

If every MG controls its generators and ESs to follow the above target value, then it is easy to show that $\sum_{n\in N_1}\mu_{n,t}^p$ equals Z_t^p, i.e., the aggregated power exchange target matches the required power support. Similarly, the ratio and local target power exchange for reactive power can be defined in (4) and (5), respectively. In this paper, we assume the reactive power is generated by dispatchable DGs [23], [24]. However, this assumption can be changed according to the operation criteria.

$$\lambda_t^q = \frac{Z_t^q - \sum_{n\in N_1}\left(\sum_{i\in G_n} Q_{i,t} - \sum_{i\in D_{1n}\cup D_{2n}}\left(L_{i,t}^Q + Q_{i,t}^D\right)\right)}{\sum_{n\in N_1}\sum_{i\in G_n}\delta_i^q} \quad (4)$$

$$\mu_{n,t}^q = \sum_{i\in G_n} Q_{i,t} + \lambda_t^q\sum_{i\in G_n}\delta_i^q - \sum_{i\in D_{1n}\cup D_{2n}}\left(L_{i,t}^Q + Q_{i,t}^D\right). \quad (5)$$

If $\mu < 0$, then the current aggregated power exchange from normal-operation MGs exceeds the required power support. The generators should decrease the output and the ESs should be operated in the charging or idle mode. Without loss of generality, this paper will focus on the situation with $\mu > 0$. λ can be used in the local power exchange computation in each normally-operating MG. It can be seen from (3) that the MG with more adjustable capacity will take more power-support allocation. A centralized approach can be used for the generation dispatch of MGs. However, it will suffer from many problems such as high-communication infrastructure costs and low reliability. Alternatively, a distributed technique can be applied in which the power exchange target $\mu_{n,t}$ is computed locally at each MG via information exchange only with its neighboring MGs.

It is of note that all terms in (2) are the same for all MGs. Hence, they can be considered as a consensus agreement that all MGs reach [18], [20]. The average consensus algorithm [18], [19] can be applied to compute the ratio λ iteratively. In the consensus algorithm, the iteration variable can be linearly updated as follows:

$$B_{n,t}(k+1) = B_{n,t}(k) + \tau\cdot\sum_{m\in M_n}\left(B_{m,t}(k) - B_{n,t}(k)\right). \quad (6)$$

For the calculation of active power exchange, the iteration variables are $\sum_{i\in G_n\cup E_n} P_{i,t}$, $\sum_{i\in D_{1n}\cup D_{2n}}(L_{i,t}^P + P_{i,t}^D)$ and $\sum_{i\in G_n}\delta_i^p + \sum_{i\in S_n} P_i^{\mathrm{dch,max}}$. For example, if the initial value of B is set as $B_{n,t}(0) = \sum_{i\in G_n\cup E_n} P_{i,t}$, then the value of $B_{n,t}(k)$ will converge to the average value $(1/\mathrm{card}(N_1))\sum_{n\in N_1}\sum_{i\in G_n\cup E_n} P_{i,t}$ with a proper step size. Other iteration variables can be obtained using the same procedure. After all the updates converge, the global ratio λ can be calculated locally at each MG by (2) and (4). Here, we assume the required power support Z and the total number of normally operating MGs are known to all MGs beforehand by broadcasting this information in the network [20]. The convergence of the average consensus algorithm in (6) has been extensively studied in [19] and [25] and is not a focus of this paper. In brief, the convergence is related to the eigenvalues of the Laplacian matrix representing the communication network. Thus, the topology of the network can be designed using the convergence features. The power exchange target of the nth MG $\mu_{n,t}$ can be computed locally using the ratio λ_t and (3) and (5). Compared to existing methods, the advantages of the proposed methodology can be summarized as follows.

1) It is of low complexity for communication and computation, since only local communication between neighboring MGs is involved, and scheduling is computed and conducted within each MG.
2) It protects the privacy, since only the aggregated generation and load information are visible in the upper-layer network.
3) It is fair to all MGs, since the allocated power support target for each MG is set according to its generation capacity.
4) It is reliable and resilient, since there is no central controller.

III. Problem Formulation

The main objectives in the normal operation are to minimize the operation costs, the load-control period, and the supply-demand imbalance of each MG. The general optimization problem of the nth MG in the autonomous networked MGs can be formulated as follows:

$$\min\sum_t\left(\sum_{i\in G_n} F_i\left(P_{i,t}\right) + \rho_e\left(\theta_{n,t}^p + \theta_{n,t}^q\right) + \rho_l\sum_{i\in D2_n} v_{i,t}TL_{i,t}^P\right) \quad (7)$$

$$\text{s.t.}\quad \sum_{i\in G_n\cup E_n\cup S_n} P_{i,t} + \theta_{n,t}^p = \sum_{i\in D1_n} L_{i,t}^P + \sum_{i\in D2_n} P_{i,t}^D \quad \forall t \quad (8)$$

$$\sum_{i\in G_n} Q_{i,t} + \theta_{n,t}^q = \sum_{i\in D1_n} L_{i,t}^Q + \sum_{i\in D2_n} Q_{i,t}^D \quad \forall t \quad (9)$$

Downloaded from http://iranpaper.ir
This article has been accepted for inclusion in a future issue of this journal. Content is final as presented, with the exception of pagination.

$$-\theta^{p,\max} \le \theta^{p}_{n,t} \le \theta^{p,\max} \quad \forall t \tag{10}$$

$$-\theta^{q,\max} \le \theta^{q}_{n,t} \le \theta^{q,\max} \quad \forall t \tag{11}$$

$$P^{\min}_i u_{i,t} \le P_{i,t} \le P^{\max}_i u_{i,t} \quad \forall i \in G_n, t \tag{12}$$

$$Q^{\min}_i u_{i,t} \le Q_{i,t} \le Q^{\max}_i u_{i,t} \quad \forall i \in G_n, t \tag{13}$$

$$P_{i,t} - P_{i,t-1} \le \left(2 - u_{i,t} - u_{i,t-1}\right)P^{\min}_i + \left(1 + u_{i,t-1} - u_{i,t}\right)\delta^{p}_i \quad \forall i \in G_n, t \tag{14}$$

$$P_{i,t-1} - P_{i,t} \le \left(2 - u_{i,t} - u_{i,t-1}\right)P^{\min}_i + \left(1 - u_{i,t-1} + u_{i,t}\right)\delta^{p}_i \quad \forall i \in G_n, t \tag{15}$$

$$Q_{i,t} - Q_{i,t-1} \le \left(2 - u_{i,t} - u_{i,t-1}\right)Q^{\min}_i + \left(1 + u_{i,t-1} - u_{i,t}\right)\delta^{q}_i \quad \forall i \in G_n, t \tag{16}$$

$$Q_{i,t-1} - Q_{i,t} \le \left(2 - u_{i,t} - u_{i,t-1}\right)Q^{\min}_i + \left(1 - u_{i,t-1} + u_{i,t}\right)\delta^{q}_i \quad \forall i \in G_n, t \tag{17}$$

$$-P^{\mathrm{ch},\max}_i y_{i,t} \le P_{i,t} \le P^{\mathrm{dch},\max}_i x_{i,t} \quad \forall i \in S_n, t \tag{18}$$

$$x_{i,t} + y_{i,t} \le 1 \quad \forall i \in S_n, t \tag{19}$$

$$\mathrm{SoC}_{i,t} = \mathrm{SoC}_{i,t-1} - T\left(x_{i,t}P_{i,t}\eta^{-1}_d + y_{i,t}P_{i,t}\eta_c\right)\Big/EC_i \quad \forall i \in S_n, t \tag{20}$$

$$\mathrm{SoC}_{i,t_{\min}} = \mathrm{SoC}_{i,t_{\max}} \quad \forall i \in S_n \tag{21}$$

$$\mathrm{SoC}^{\min}_i \le \mathrm{SoC}_{i,t} \le \mathrm{SoC}^{\max}_i \quad \forall i \in S_n, t \tag{22}$$

$$L^{P,\min} \le P^{D}_{i,t} \le L^{P}_{i,t} \quad \forall i \in D2_n, t \tag{23}$$

$$P^{D}_{i,t} \ge \left(1 - v_{i,t}\right)L^{P}_{i,t} \quad \forall i \in D2_n, t \tag{24}$$

$$L^{Q,\min} \le Q^{D}_{i,t} \le L^{Q}_{i,t} \quad \forall i \in D2_n, t \tag{25}$$

$$Q^{D}_{i,t} \ge \left(1 - v_{i,t}\right)L^{Q}_{i,t} \quad \forall i \in D2_n, t \tag{26}$$

$$\sum_t v_{i,t}T \le T^{c}_i \quad \forall i \in D2_n, t. \tag{27}$$

In the above formulation, the objective function (7) minimizes the operation costs and generation-demand mismatch of the nth MG. The first item in (7) represents generation costs of MTs. The generation cost can be approximated by a piecewise linear model. The second and third items represent the active and reactive power exchange of the nth MG with other MGs. In the normal operation mode, the MG should be self-adequate to ensure its supply security. The fourth item describes the total period of time with load control, i.e., $v = 1$ indicates that the corresponding time interval T is controlled. Constraints (8) and (9) are power balance equations which ensure that the sum of power generated by DGs, ESs and the power exchange with other MGs matches the total load consumption. The power outputs of MTs and ESs are control variables, while the outputs of PVs and WTs are nondispatchable. The power of ESs can be positive (discharging), negative (charging), or zero (idle). The power exchange with other MGs can be positive (generation surplus), negative (generation deficiency) or zero. Constraints (10) and (11) guarantee that the power exchange with other MGs is within the line flow limit. Constraints (12) and (13) guarantee that the power outputs of MTs are within the generation capacities. Constraints (14)–(17) represent the ramp up and ramp down limits. Constraint (18) represents the charging and discharging limits of an ES according to its operation mode. For example, $x = 1$ and $y = 0$ represents the discharging mode of the ES and the maximum discharging limits are imposed. Constraint (19) guarantees that the ES works in only one mode at a certain time. Constraint (20) represents the SoC of an ES. Constraint (21) guarantees the ES has the same SoC at the beginning and the end of the scheduling horizon. Constraint (22) represents the limit of SoC. Constraints (23)–(26) describe the power consumption of the controllable load. For example, if $v = 1$, which indicates load control is applied, constraints (23) and (25) are imposed, while constraints (24) and (26) become redundant. In constraint (27), when load is controlled, the associated state v is one; it is zero otherwise. The aggregated load-control time should not exceed the maximum allowable value.

When a generation deficiency or fault happens, the system switches to the self-healing stage. In the self-healing mode, the on-fault MG or MGs will receive power support from other MGs by optimally scheduling the power exchanges and redispatching the controllable DGs and ESs according to the local target power exchange value μ. The operation problem of the nth MG without faults can be formulated as

$$\min\left(\theta^{p}_{n,t} - \mu^{p}_{n,t}\right)^2 + \left(\theta^{q}_{n,t} - \mu^{q}_{n,t}\right)^2 \text{ s.t. } (8)-(27). \tag{28}$$

The operation objective in (28) is to make the power exchange with the common point approach μ as closely as possible. The self-healing problem is further subject to power balance constraints, power transfer constraints, dispatchable DG generation and ramp limits, and ES operation limits. It is of note that the above formulation (28) applies to MGs under normal operation. We also set $v = 0$ to indicate that loads in MGs without an emergency should not be sacrificed to support the on-emergency MG or MGs.

In sum, the problem formulated in (7)–(27) is for the normal operation mode and the problem formulated in (28) is for the self-healing mode. Both are mix-integer linear programming (MILP) problems and can be solved by commercial solvers, such as DICOPT [26].

IV. Numerical Results

The proposed method has been examined on a system with six MGs as shown in Fig. 2. The information of DGs, ESs, and loads is summarized in Tables I–IV. We assume that each bus within an MG shares the same amount of load. It is assumed that the predicted loads are the products of total loads shown in Table IV and multipliers shown in Fig. 3. The outputs of renewable DGs are assumed to be the products of sizes in Table III and the corresponding multipliers in Fig. 4. The multipliers are used to make load and generation profiles change with time [27]. $P^{\min}$ and $Q^{\min}$ are set to be zero for all MTs. δ^p and δ^q are set to be 50% of $P^{\max}$ and $Q^{\max}$, respectively. $\mathrm{SoC}^{\max}$ and $\mathrm{SoC}^{\min}$ are set to be 0.9 and 0.2, respectively. The initial SoC is set to be 0.65 for all ESs. η_d and η_c are set to be 0.95 for all ESs. The minimum active and reactive demand of a controllable load is 10% of its load size. The maximum allowed control time is 6 h for all loads. A 1-h time step is used in simulations. All the above settings are for illustration and can be changed according to the availability of system data. The experiment is implemented on a computer with Intel Core i5 3.30 GHz with 4 GB memory and GAMS 23.4. The computation time of all cases is within 3 s.

Downloaded from http://iranpaper.ir
This article has been accepted for inclusion in a future issue of this journal. Content is final as presented, with the exception of pagination.

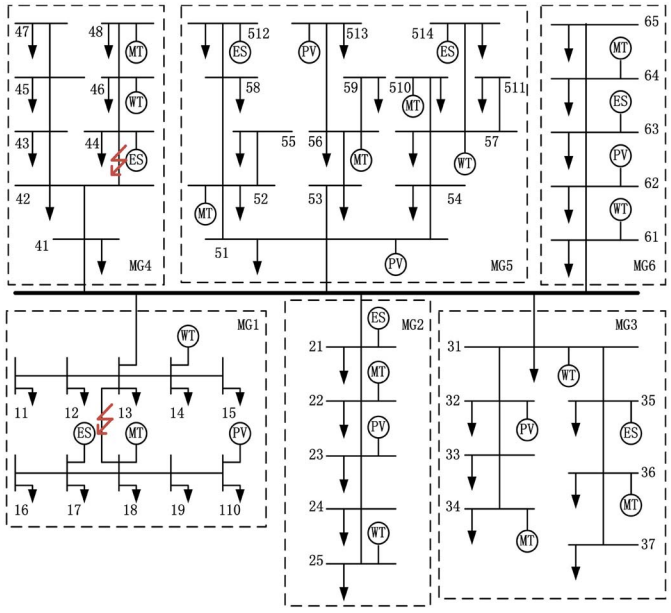

Fig. 2. Test system with six networked MGs.

TABLE I
LOCATIONS AND SIZES OF MTS

Bus #	a ($/MW^2)	b ($/MW)	c ($)	P^{max} (MW)	Q^{max} (MW)	δ^p (MW/h)	δ^p (MVAR/h))
18	0.0696	26.244	31.67	8	6	2.5	2.0
22	0.0288	37.697	17.95	4	2	1.5	1.0
34	0.0468	40.122	22.02	2	2	0.5	0.5
36	0.0288	37.697	21.95	4	2	1.5	0.5
48	0.0468	40.122	22.02	8	3	2.0	1.0
52	0.0288	30.697	21.95	4	3	1.5	1.0
56	0.0681	12.441	32.01	6	4	2.5	1.5
510	0.0268	30.122	22.02	4	3	1.5	1.0
64	0.0288	37.697	21.95	8	3	2.0	1.0

TABLE II
LOCATIONS AND SIZES OF PVS AND WTS

MG #	Bus #	Type	P^{max} (MW)
MG1	14	WT	2
	110	PV	1.5
MG2	23	PV	1
	25	WT	1
MG3	31	WT	1
	32	PV	0.5
MG4	46	WT	3
MG5	57	WT	2
	513	PV	1
MG6	61	WT	1
	62	PV	1

It is assumed that the six MGs are connected via a ring cyber network. The step τ in the consensus algorithm can be calculated as $\tau = 2/[\varphi_2(L) + \varphi_N(L)]$, where L is the Laplacian matrix representing the graph and $\varphi_i(L)$ is the ith smallest eigenvalue of the graph Laplacian matrix [20]. Thus, the step size of the consensus algorithm in this paper can be calculated as $\tau = 2/[\varphi_2(L) + \varphi_6(L)] = 0.4$, where the second smallest eigenvalue of Laplacian matrix of the ring cyber network with six MGs is 1.0 and the six smallest one is 4.0.

TABLE III
LOCATIONS AND CAPACITIES OF ESS

Bus #	Capacity (MWh)	$P^{ch,max}$ (MW)	$P^{dch,max}$ (MW)
17	5	1	1
21	2	0.4	0.4
35	2	1.2	1.2
44	4	0.6	0.6
512	1	0.2	0.2
514	2	0.4	0.4
63	1	0.2	0.2

TABLE IV
LOAD INFORMATION

MG#	Total Active Load (MW)	Total Reactive Load (MVAR)	Bus# of Controllable Load
MG1	10	3	16, 19
MG2	5	1.5	21, 22, 24
MG3	7	2.1	32, 37
MG4	8	2.4	44, 46
MG5	12.6	2.8	53, 59, 512
MG6	5	1.5	61, 65

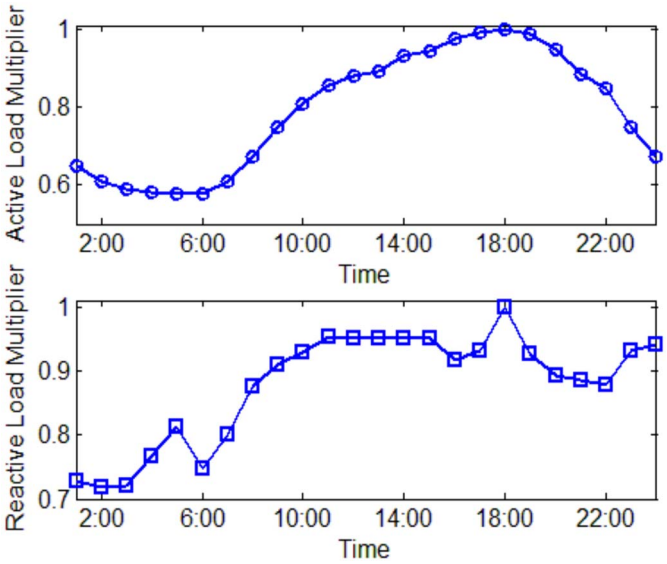

Fig. 3. Load profile multiplier.

A. Case 1: Normal Operation Mode:

This case demonstrates the optimal scheduling of each MG for a 24-h horizon. In the normal operation mode, each MG works independently to minimize its operation costs and ensure the self-adequacy as shown in the formulations (7)–(27). The unit commitment states of MTs are shown in Table V.

Figs. 5 and 6 present the optimal generation schedules of active power and reactive power, respectively. Fig. 7 shows the schedules of ESs. No load control is necessary. Take MG3 as an example, the MT34 is off in the first 6 h due to its higher generation cost compared to MT36 and the fact that the supply-demand balance can be met by WTs, PVs, and MT36. MT36 will reach its maximum capacity firstly, and the remaining generation-load gap will be filled by MT34. The ES will be committed to discharge power when outputs of WTs and PVs

Downloaded from http://iranpaper.ir
This article has been accepted for inclusion in a future issue of this journal. Content is final as presented, with the exception of pagination.

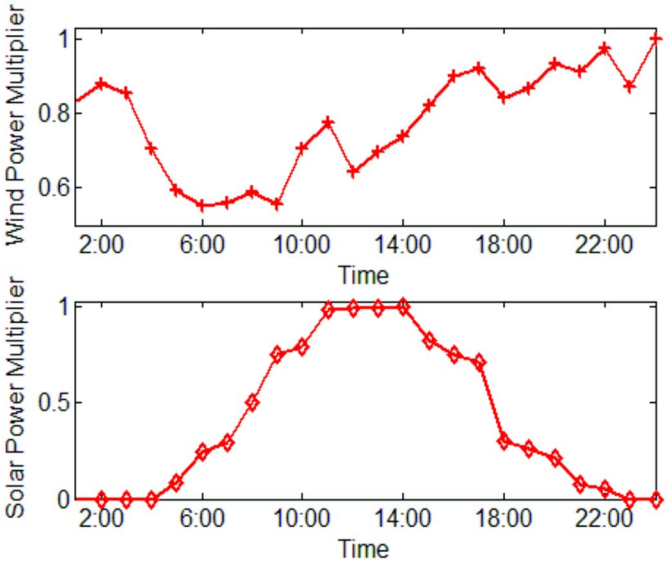

Fig. 4. Predicted wind and solar power multipliers.

TABLE V
MT COMMITMENT STATES IN CASE 1

	Hours (1-24)																							
MT18	1	1	1	1	1	1	1	1	1	1	1	1	1	1	1	1	1	1	1	1	1	1	1	1
MT22	1	1	1	1	1	1	1	1	1	1	1	1	1	1	1	1	1	1	1	1	1	1	1	1
MT34	0	0	0	0	0	0	1	1	1	1	1	1	1	1	1	1	1	1	1	1	1	1	1	1
MT36	1	1	1	1	1	1	1	1	1	1	1	1	1	1	1	1	1	1	1	1	1	1	1	1
MT48	1	1	1	1	1	1	1	1	1	1	1	1	1	1	1	1	1	1	1	1	1	1	1	1
MT52	0	0	0	0	0	0	0	1	1	1	1	1	1	1	1	1	1	1	1	1	1	1	1	0
MT56	1	1	1	1	1	1	1	1	1	1	1	1	1	1	1	1	1	1	1	1	1	1	1	1
MT510	1	1	0	0	0	1	1	1	1	1	1	1	1	1	1	1	1	1	1	1	1	1	1	1
MT64	1	1	1	1	1	1	1	1	1	1	1	1	1	1	1	1	1	1	1	1	1	1	1	1

Note: The number after MT represents the installation bus, e.g., MT18 represents the MT at bus 18.

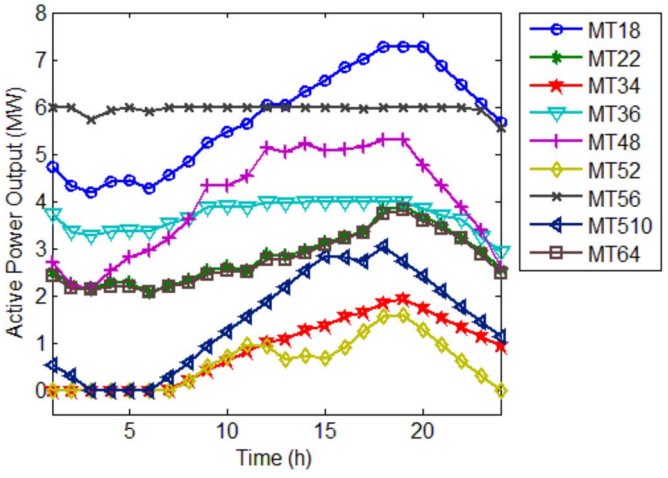

Fig. 5. Active power output of MTs in Case 1.

suffer from sudden drop and large generation ramp-up is necessary around 18:00. Similarly in MG5, MT52 is always committed. MT56 and MT510 are committed when there is a large generation-load gap or MT52 reaches its capacity limit.

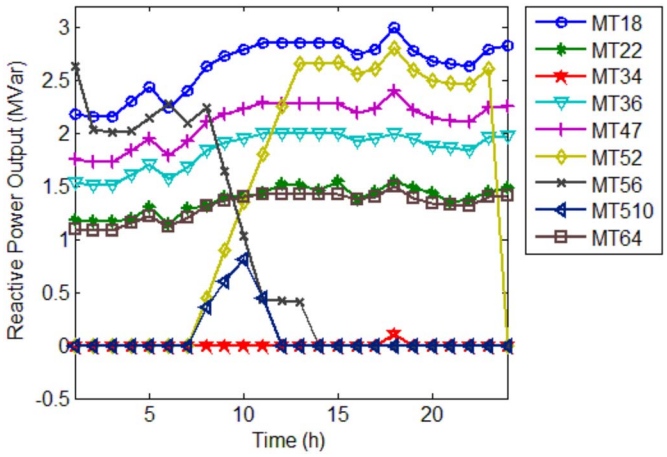

Fig. 6. Reactive power output of MTs in Case 1.

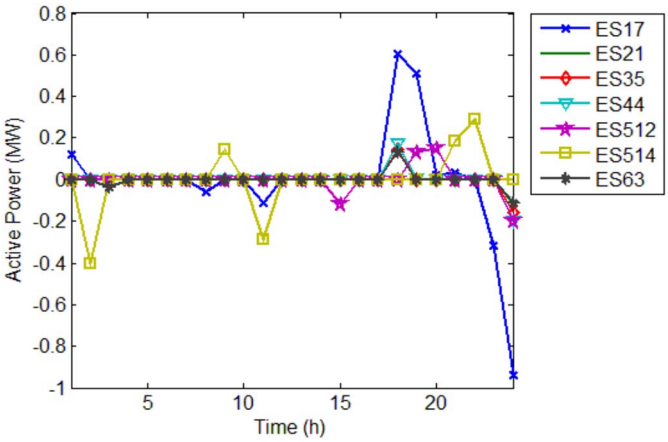

Fig. 7. Power output of ESs (negative-charging, positive-discharging, and zero-idle).

B. Case 2: Self-Healing With Single Fault:

In this case, we assume that a single fault happens on the line sections 13–18 in MG1 at 18:00 as shown in Fig. 2. For illustration, it is assumed that the fault will be cleared in 2 h [28] and the analysis is performed for two time points 18:00 and 19:00 as an example. At 18:00, the total load at buss 11–14 is 5 MW and 1.5 MVAR, the output of WT is 1.682 MW. To ensure the power supply of loads at buses 11–14, the requested power support is 3.3188 MW and 1.5 MVAR. The requested power support at 19:00 is 3.2110 MW and 1.3884 MVAR, which are calculated in the same way. The allocation of the power support can be computed in a distributive way as discussed in Section II. Fig. 8 shows the iteration of $\sum_{n\in N_1}\sum_{i\in G_n\cup E_n} P_{i,t}$ at 18:00 for MGs without faults.

Each MG starts the iteration with its own total generation, and exchanges information with its neighboring MGs in the ring-connected cyber network. The algorithm converges to the same value 5.963 MW, which is the averaged generation of all normally-operating MGs, in 14 iterations. At the beginning, each MG only knows its own generation; at the end, each MG knows that the total active generation of all normally-operating MGs at this point in time is 29.815 MW. It is of

Downloaded from http://iranpaper.ir
This article has been accepted for inclusion in a future issue of this journal. Content is final as presented, with the exception of pagination.

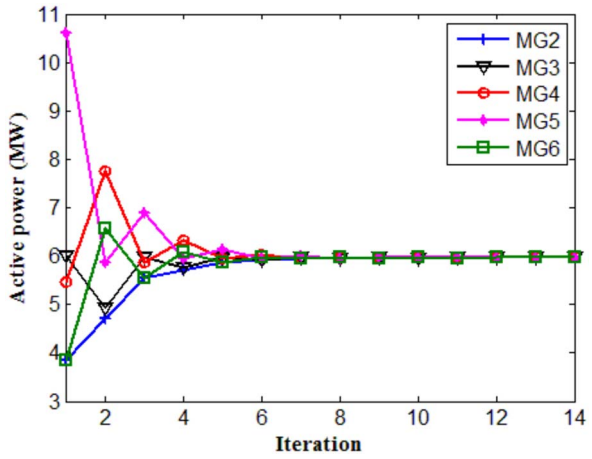

Fig. 8. Iteration of total active power output of DGs in all normally-operating MGs at 18:00.

TABLE VI
REDISPATCH RESULTS OF MTS AND ESS IN CASE 2

	MT22 (MW)	MT34 (MW)	MT36 (MW)	MT47 (MW)	MT52 (MW)	MT56 (MW)	MT510 (MW)	MT64 (MW)
18:00	4	1.863	4	5.591	1.685	6	3.807	3.774
19:00	4	1.787	4	5.512	1.6	6	3.723	3.895
	MT22 (MVAR)	MT34 (MVAR)	MT36 (MVAR)	MT47 (MVAR)	MT52 (MVAR)	MT56 (MVAR)	MT510 (MVAR)	MT64 (MVAR)
18:00	1.603	2	0.41	2.555	3	0.126	0.45	1.655
19:00	1.484	2	0.231	2.365	2.952	0.199	0.16	1.532
	ES21 (MW)	ES35 (MW)	ES44 (MW)	ES512 (MW)	ES514 (MW)	ES63 (MW)		
18:00	0.323	1.164	0.181	0.2	0.4	0.147		
19:00	0.295	1.148	0	0.2	0.4	0		

note that the converged average generation is not the target generation; instead, it will be used to calculate the allocated support. The values of $\sum_{i\in D_{1n}\cup D_{2n}}(L^P_{i,t}+P^D_{i,t})$ and $\sum_{i\in G_n}\delta^p_i+\sum_{i\in S_n}P^{\text{dch,max}}_i$ can be calculated in the similar way. Finally, each MG can calculate λ^p_t according to (2). In this case, $\lambda^p_t=2.0112$ at 18:00. The allocated power support for each MG can be calculated using (3).

Table VI shows the redispatch results of MTs and ESs. For example, MT22 ramps to its maximum capacity to provide power support allocated to MG2. In the normal operation in Case 1, the total generation cost at 18:00 and 19:00 is \$2695.4; in the self-healing mode in Case 2, the total generation cost during the same period is \$2788.3. The cost increases by \$92.9, which is due to the increased generation to support the on-fault MG.

Fig. 9 presents the allocated power support and the actual power support after reschedule. It can be seen that the scheduled power support of each MG matches the allocated power support, which implies that the aggregated scheduled power support matches the requested one.

C. Case 3: Self-Healing With Multiple Faults

In this case, we test the performance of the proposed method with multiple faults in different MGs. It is assumed that two faults happen in the networked-MG system at 3:00 A.M.: one is in the line sections 13–18 in MG1 and the other is in the line sections 42–44 in MG4. The two on-emergency MGs

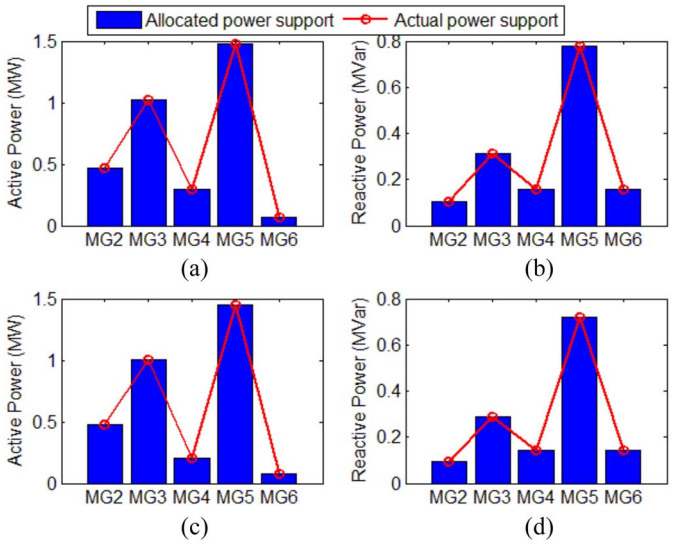

Fig. 9. Allocated power support request and actual power support of each MG in Case 2. (a) and (b) Active and reactive power support at 18:00, respectively. (c) and (d) Active and reactive power support at 19:00, respectively.

TABLE VII
REDISPATCH RESULTS OF MTS AND ESS IN CASE 3

	MT22 (MW)	MT34 (MW)	MT36 (MW)	MT52 (MW)	MT56 (MW)	MT510 (MW)	MT64 (MW)
3:00	2.488	1.546	1.92	0.32	6	0.837	2.477
4:00	2.646	1.346	2.32	0.64	6	0.64	2.606
	MT22 (MVAR)	MT34 (MVAR)	MT36 (MVAR)	MT52 (MVAR)	MT56 (MVAR)	MT510 (MVAR)	MT64 (MVAR)
3:00	1.248	0.374	1.64	0.45	0.352	2.46	1.331
4:00	1.336	0.574	1.595	0.90	0.424	2.095	1.429
	ES21 (MW)	ES35 (MW)	ES512 (MW)	ES514 (MW)	ES63 (MW)		
3:00	0.4	1.014	0	0.4	0		
4:00	0.4	0.931	0.158	0.4	0.054		

will receive support from MG2, MG3, MG5, and MG6. At 3:00 A.M., the requested power support is 4.1959 MW and 2.1621 MVAR; at 4:00 A.M., the requested power support is 4.4174 MW and 2.2989 MVAR. Table VII presents the reschedule results of MTs and ESs. The total generation cost at 3:00 and 4:00 A.M. in Case 1 is \$1574.1; the total generation cost during the same period in Case 3 is \$1735.5, which is \$161.4 more than that in the normal operation mode.

Fig. 10 shows that the actual power support after redispatch matches the allocated power the support, which implies that the aggregated scheduled power support meets the requested one.

D. Case 4: Self-Healing of 40 MGs

In order to further verify the proposed architecture, we test the performance of the proposed method in a network with 40 MGs connected with a common bus. Among the 40 MGs, there are four configuration types which are the same as MG1, MG2, MG4, and MG5 in Fig. 2, respectively. Each configuration type has ten MGs. The EMSs of MGs are connected via a ring cyber network. For illustration, we assume that five of MG1-type MGs have the same fault locations as shown

Downloaded from http://iranpaper.ir
This article has been accepted for inclusion in a future issue of this journal. Content is final as presented, with the exception of pagination.

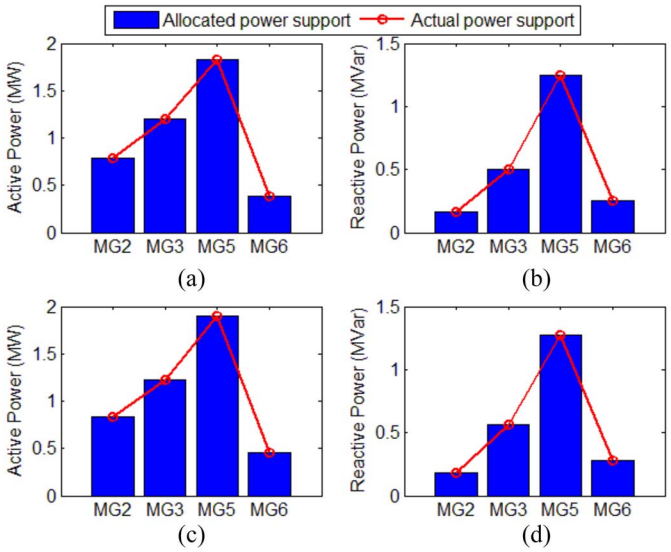

Fig. 10. Allocated power support request and actual power support of each MG in Case 2. (a) and (b) Active and reactive power support at 3:00, respectively (c) and (d) Active and reactive power support at 4:00, respectively.

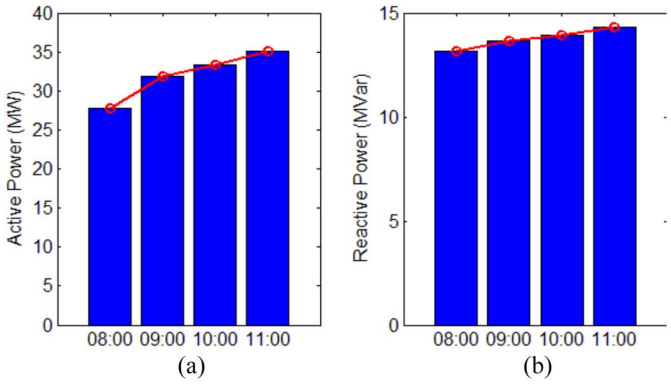

Fig. 11. Total required and aggregated scheduled (a) active and (b) reactive power support.

in Fig. 2, and five of MG4-type MGs have the same fault locations as shown in Fig. 2. It is also assumed that the faults happen at 8:00 A.M. and are cleared at 11:00 A.M. Fig. 11 shows the total required power support and actual aggregated scheduled power support meets each other during the fault periods.

V. Conclusion

In this paper, we present a novel methodology for the optimal operation and self-healing of networked MGs. In the normal operation mode, each MG operates independently to fulfill its own objective. In the self-healing mode, the on-emergency MG receives local power support from other MGs. A two-layer cyber communication and control protocol is proposed to allocate the requested power support to each MG in a decentralized way, where an EMS only communicates with its neighboring EMSs. The proposed methodology has the following notable advantages.

1) The self-adequate networked MGs can improve the system operation, self-healing, and reliability.
2) The decentralized cyber communication and control method is of lower cyber infrastructure costs and higher reliability compared to a centralized method.
3) The privacy of each MG is respected since only information on aggregated power is visible in the upper-layer cyber network.

Case studies on systems with networked MGs show that the proposed technique can improve the development of an intelligent and resilient power distribution system. Future research directions include economic considerations and dynamic stability issues in providing power support in the self-healing mode.

References

[1] A. Khodaei, "Microgrid optimal scheduling with multi-period islanding constraints," *IEEE Trans. Power Syst.*, vol. 29, no. 3, pp. 1383–1392, May 2014.
[2] Z. Wang, B. Chen, J. Wang, M. Begovic, and C. Chen, "Coordinated energy management of networked microgrids in distribution systems," *IEEE Trans. Smart Grid*, vol. 6, no. 1, pp. 45–53, Jan. 2015.
[3] S. A. Arefifar, Y. A.-R. I. Mohamed, and T. H. M. El-Fouly, "Comprehensive operational planning framework for self-healing control actions in smart distribution grids," *IEEE Trans. Power Syst.*, vol. 28, no. 4, pp. 4192–4200, Nov. 2013.
[4] A. K. Marvasti, Y. Fu, S. DorMohammadi, and M. Rais-Rohani, "Optimal operation of active distribution grids: A system of systems framework," *IEEE Trans. Smart Grid*, vol. 5, no. 3, pp. 1228–1237, May 2014.
[5] S. A. Arefifar, Y. A.-R. I. Mohamed, and T. H. M. El-Fouly, "Optimum microgrid design for enhancing reliability and supply-security," *IEEE Trans. Smart Grid,* vol. 4, no. 3, pp. 1567–1575, Sep. 2013.
[6] A. Kargarian, B. Falahati, F. Yong, and M. Baradar, "Multiobjective optimal power flow algorithm to enhance multi-microgrids performance incorporating IPFC," in *IEEE Power Energy Soc. Gen. Meeting*, San Diego, CA, USA, 2012, pp. 1–6.
[7] J. Wu and X. Guan, "Coordinated multi-microgrids optimal control algorithm for smart distribution management system," *IEEE Trans. Smart Grid*, vol. 4, no. 4, pp. 2174–2181, Dec. 2013.
[8] G. E. Asimakopoulou, A. L. Dimeas, and N. D. Hatziargyriou, "Leader–follower strategies for energy management of multi-microgrids," *IEEE Trans. Smart Grid*, vol. 4, no. 4, pp. 1909–1916, Dec. 2013.
[9] M. Fathi and H. Bevrani, "Adaptive energy consumption scheduling for connected microgrids under demand uncertainty," *IEEE Trans. Power Del.*, vol. 28, no. 3, pp. 1576–1583, Jul. 2013.
[10] Z. Wang, B. Chen, J. Wang, J. Kim, and M. Begovic, "Robust optimization based optimal DG placement in microgrids," *IEEE Trans. Smart Grid*, vol. 5, no. 5, pp. 2173–2182, Sep. 2014.
[11] A. Khodaei and M. Shahidehpour, "Microgrid-based co-optimization of generation and transmission planning in power systems," *IEEE Trans. Power Syst.*, vol. 28, no. 2, pp. 1582–1590, May 2013.
[12] Q. Jiang, M. Xue, and G. Geng, "Energy management of microgrid in grid-connected and stand-alone modes," *IEEE Trans. Power Syst.*, vol. 28, no. 3, pp. 3380–3389, Aug. 2013.
[13] W. Su and J. Wang, "Energy management systems in microgrid operations," *Elect. J.*, vol. 25, no. 8, pp. 45–60, Oct. 2012.
[14] W. Su, J. Wang, and J. Roh, "Stochastic energy scheduling in microgrids with intermittent renewable energy resources," *IEEE Trans. Smart Grid*, vol. 5, no. 4, pp. 1876–1883, Jul. 2014.
[15] C. Moreira, F. Resende, and J. P. Lopes, "Using low voltage microgrids for service restoration," *IEEE Trans. Power Syst.*, vol. 22, no. 1, pp. 395–403, Feb. 2007.
[16] *IEEE Guide for Design, Operation, and Integration of Distributed Resource Island Systems with Electric Power Systems*, IEEE Standard 1547.4, 2011, pp. 1–54.
[17] Z. Wang and J. Wang, "Self-healing resilient distribution systems based on sectionalization into microgrids," *IEEE Trans. Power Syst.* [Online]. Available: http://ieeexplore.ieee.org/xpl/articleDetails.jsp?tp=&arnumber=7017458
[18] A. D. Dominguez-Garcia and C. N. Hadjicostis, "Distributed algorithms for control of demand response and distributed energy resources," in *Proc. 50th IEEE Conf. Decis. Control Eur. Control Conf. (CDC-ECC)*, 2011, pp. 27–32.

Downloaded from http://iranpaper.ir
This article has been accepted for inclusion in a future issue of this journal. Content is final as presented, with the exception of pagination.

[19] A. D. Dominguez-Garcia, C. N. Hadjicostis, and N. F. Vaidya, "Resilient networked control of distributed energy resources," *IEEE J. Sel. Areas Commun.*, vol. 30, no. 6, pp. 1137–1148, Jul. 2012.
[20] C. Chen, J. Wang, and S. Kishore, "A distributed direct load control approach for large-scale residential demand response," *IEEE Trans. Power Syst.*, vol. 29, no. 5, pp. 2219–2228, Sep. 2014.
[21] Silver Spring Networks. (2013). *Our Network Smart Grid Infrastructure: Ensuring System Connectivity*. [Online]. Available: http://www.silverspringnet.com/products/network-infrastructure/
[22] H. S. V. S. K. Nunna and S. Doolla, "Multiagent-based distributed-energy-resource management for intelligent microgrids," *IEEE Trans. Ind. Electron.*, vol. 60, no. 4, pp. 1678–1687, Apr. 2013.
[23] *IEEE Standard for Interconnecting Distributed Resources With Electric Power Systems*, IEEE Standard 1547, 2003, pp. 1–28.
[24] H. Li, F. Li, Y. Xu, D. T. Rizy, and S. Adhikari, "Autonomous and adaptive voltage control using multiple distributed energy resources," *IEEE Trans. Power Syst.*, vol. 28, no. 2, pp. 718–730, May 2013.
[25] A. D. Dominguez-Garcia and C. N. Hadjicostis, "Coordination and control of distributed energy resources for provision of ancillary services," in *Proc. 1st IEEE Int. Conf. Smart Grid Commun. (SmartGridComm)*, Gaithersburg, MD, USA, 2010, pp. 537–542.
[26] I. E. Grossmann, J. Viswanathan, A. Vecchietti, R. Raman, and E. Kalvelagen, "GAMS/DICOPT: A discrete continuous optimization package," *Math. Methods Appl. Sci.*, vol. 24, no. 11, pp. 649–664, Jul. 2001.
[27] Z. Wang, B. Chen, J. Wang, M. Begovic, and Y. He, "MPC-based Voltage/VAR optimization for distribution circuits with distributed generators and exponential load models," *IEEE Trans. Smart Grid*, vol. 5, no. 5, pp. 2412–2420, Sep. 2014.
[28] A. Zidan and E. F. El-Saadany, "A cooperative multiagent framework for self-healing mechanisms in distribution systems," *IEEE Trans. Smart Grid*, vol. 3, no. 3, pp. 1525–1539, Sep. 2012.

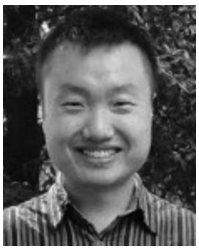

Zhaoyu Wang (S'13) received the B.S. degree in electrical engineering from Shanghai Jiaotong University, Shanghai, China, in 2009, and the M.S. degrees in electrical engineering from Shanghai Jiaotong University, and in electrical and computer engineering from the Georgia Institute of Technology, Atlanta, GA, USA, in 2012. He is currently pursuing the Ph.D. degree with the School of Electrical and Computer Engineering, Georgia Institute of Technology.

In 2013, he was a Research Aide Intern with the Decision and Information Sciences Division, Argonne National Laboratory, Argonne, IL, USA. In 2014, he was an Electrical Engineer with Corning Inc., Corning, NY, USA. His current research interests include microgrids, volt/VAR control, self-healing resilient power grids, and demand response and energy conservation.

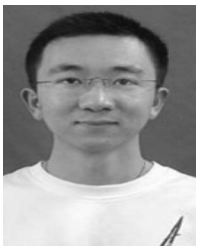

Bokan Chen received the B.S. degree in electronics and information engineering from the Huazhong University of Science and Technology, Wuhan, China, in 2011, and the M.S. degree from the Department of Industrial and Manufacturing Systems Engineering, Iowa State University, Ames, IA, USA, where he is currently pursuing the Ph.D. degree.

His current research interests include optimization theories and their applications.

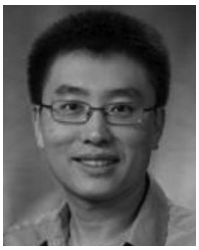

Jianhui Wang (M'07–SM'12) received the Ph.D. degree in electrical engineering from the Illinois Institute of Technology, Chicago, IL, USA, in 2007.

He is currently the Section Lead of Advanced Power Grid Modeling with the Energy Systems Division, Argonne National Laboratory, Argonne, IL. He is also an Affiliate Professor with Auburn University, Auburn, AL, USA, and an Adjunct Professor with the University of Notre Dame, Notre Dame, IN, USA.

Dr. Wang is the Editor-in-Chief of the IEEE TRANSACTIONS ON SMART GRID, and a Distinguished Lecturer of the IEEE Power and Energy Society (PES). He is the Secretary of the IEEE PES Power System Operations Committee.

Chen Chen (S'10–M'13) received the B.S. and M.S. degrees from Xi'an Jiaotong University, Xi'an, China, in 2006 and 2009, respectively, and the Ph.D. degree from Lehigh University, Bethlehem, PA, USA, in 2013, all in electrical engineering.

He is currently a Postdoctoral Researcher with the Energy Systems Division, Argonne National Laboratory, Argonne, IL, USA. His current research interests include optimization, communications, and signal processing for smart electricity systems.